Probability imaging of binary stars from infrared speckle observations

M. Carbillet, E. Aristidi, G. Ricort and C. Aime

Département d'Astrophysique de l'Université de Nice-Sophia Antipolis
Unité de Recherche Associée 709 du Centre National de la Recherche Scientifique
Parc Valrose, 06108 Nice Cedex 2, France

ABSTRACT

We report in this communication experimental results obtained by the technique of Probability Imaging applied to double stars in the near-infrared. Intensity ratios and relative positions of components are obtained for six double stars. The two-fold probability density function of one-dimensional images is used to reconstruct the binary system. The data reduction is made with a parametric approach, by minimizing a distance between observed two-fold probability density functions and modelled ones, obtained by using a close-by reference star.

1 INTRODUCTION

This communication presents a practical implementation of the technique of Probability Imaging (PI) to the image reconstruction of binary systems from one-dimensional near-infrared specklegrams. It follows the work of Aime et al.[4] who first used PI to the image reconstruction of ζ *Aqr*. The present approach uses a data reduction procedure that makes it possible to obtain quantitative results suitable for astrophysical interpretations.

The infrared data processed here were obtained by Ch. Perrier in K band ($\lambda = 2.2\ \mu, \Delta\lambda = 0.39\ \mu$) on December 1987 and March 1991 with the ESO slit-scanning infrared specklegraph attached to the 3.60 m telescope, the diffraction limit being in this conditions $0\farcs140$.

PI technique belongs to the speckle imaging techniques invented by Labeyrie[11] and that use a statistical analysis to recover images at high angular resolution in spite of atmospheric turbulence. It may be compared to the techniques of Knox and Thompson[9] and to speckle masking[19] .

PI is based on the study of the probability density function (PDF) at several points in space of the speckle pattern that is formed at the focus of the telescope. As shown by Aime[1] , all the parameters of a binary system, i.e. the star separation, relative amplitude and position of the components can be derived from the analysis of the two-fold PDF of the speckle pattern. The present study develops an improved data reduction approach using minimization techniques to obtain these parameters with a high accuracy.

The communication is organized as follows. A brief summary of the principle of PI and its application to the imaging of a binary system is given in section 2. The procedure to quantitatively determine the parameters of the binary systems, by means of comparison between two-fold PDFs of observed and synthesized one-dimensional images of double star speckle patterns, is described in section 3. The infrared results obtained on the double stars

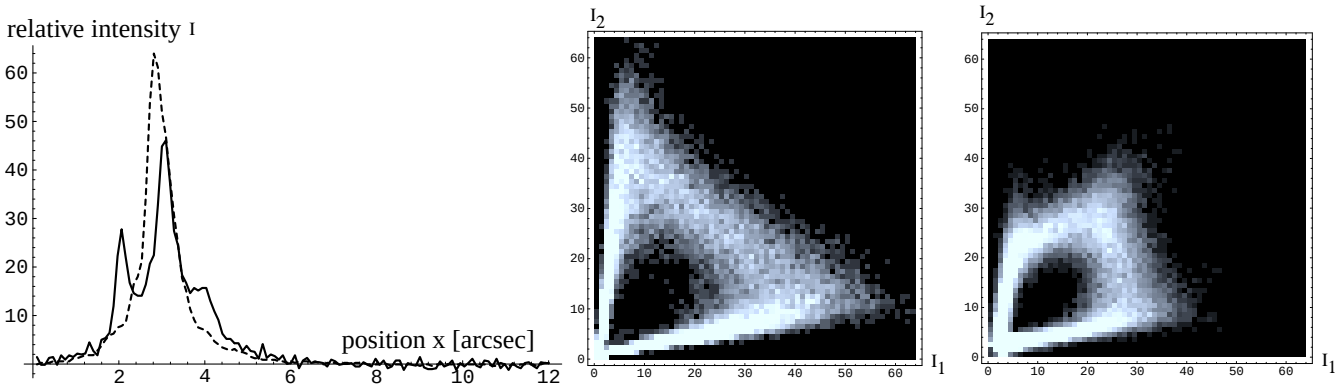

Figure 1: Example of scans and two-fold PDFs : $P(I_1, I_2; \rho = 10$ pixels $[0''.938])$, for the point source-like reference single star $\alpha\ Aqr$ and for the double star $\zeta\ Aqr$. A scan of $\alpha\ Aqr$ is represented in dashed line,while one of $\zeta\ Aqr$ is in full line. The calculation of the two-fold PDFs was made from a set of 757 scans for $\zeta\ Aqr$ and 732 scans for $\alpha\ Aqr$, obtained on December $10th$ 1987, in a West to East scanning direction. The variation in intensity of the signal is restricted to 64 integer values. The discretization sample in intensity used here is the same for the two sets of data.

$\zeta\ Aqr$, $\gamma\ Vir$, $\zeta\ Ori$, Gl 473, Gl 866 and Gl 804 are also given in section 3. A discussion including the further possible improvements of the procedure is made in section 4.

2 PRINCIPLE OF PROBABILITY IMAGING OF A DOUBLE STAR

A binary system, for which none of the stars is individually resolved by the telescope, is the simplest object that can be considered for image reconstruction. Its perfect image is made of two points of intensities b_1 and b_2, separated by a vector of position $\underline{d}$. In a one-dimensional analysis, we can only obtain the projection d of $\underline{d}$ onto a direction of the sky ; the recovery of $\underline{d}$ remains possible by performing analysis in two different scanning directions, as we shall see for the star Gl 473. Unless a very accurate photometry is performed, we cannot access the absolute values b_1 and b_2, but only their ratio $\alpha = b_2/b_1$.

The object of our analysis will be therefore to obtain these two quantities d and α. It is important to note that α, whether its value is lower or greater then 1, will give the relative positions of the stars, a quantity that cannot be obtained using Labeyrie's speckle interferometry technique. We shall now briefly summarize how the PI technique may give the values of d and α.

For the intensity $I(x)$ of a one-dimensional speckle image, the quantity $P(I_1, I_2; \rho)\, dI_1\, dI_2$ measures the probability that $I(x)$ has an intensity value lying in the elementary interval $\{I_1, I_1 + dI_1\}$ while $I(x + \rho)$, of the same scan, has an intensity value lying in the interval $\{I_2, I_2 + dI_2\}$. The quantity $P(I_1, I_2; \rho)$, function of the three variables I_1, I_2 and ρ, is the two-fold PDF of $I(x)$.

As discussed by Aime et al.[4] , there is a strong difference between two-fold PDFs of speckle patterns produced by a point source and a double star. For a given value of ρ, the observed PDFs appears as joint occurence histograms of the discretized values I_1 and I_2, and can be represented as gray-level images (cf. Figure 1).

For the point source speckle patterns, these figures are symmetrical in I_1 and I_2, whatever the value of ρ ; for

the double star, the PDF shows a dissymetric structure for the values of ρ close to the star separation d. The principle of PI is based on the fact that there is an unique relationship between the shape of the two-fold PDF and the ratio of components α.

The drawback of the PI technique is that this relationship cannot be simply expressed as the product of a function that depends on d and α alone and a function that is relevant to the point source speckle pattern. This makes calibration of the results difficult. Different approaches have already been investigated to overcome this difficulty (Aime and Aristidi[3] , Aime[2]). For the present analysis, we have choosen to use an improved version of the calibration procedure of experimental and numerical nature which was proposed by Aime et al.[4] ; its implementation is described in the next section.

3 CALIBRATION PROCEDURE

For the ESO slit-scanning specklegraph, the data are made of one-dimensional scans $I(x)$, representing the projection of the two-dimensional speckle image onto the scanning direction (Perrier[14]). Each observation resulted in two sets of scans : one on the double star and the other one on its reference star. Each scan is made up of 128 data points, the first 64 corresponding to the scanning of the star speckle pattern itself, the remaining part of the scan being done on the sky for noise background analysis.

3.1 Practical implementation of the comparison between observed and synthesized PDFs

The procedure we use to synthesize the two-fold PDF of a possible observed double star is an improvement of the one proposed by Aime et al.[4] . It basically consists of constructing, from the set of reference point source speckle patterns $\{S_i(x)\}_{i=1,N}$, a set of speckle images $\{D_i^{d,\alpha}(x)\}_{i=1,N}$, that may be representative of the speckle patterns which would be observed for a binary star of angular separation d and intensity ratio α. We expect that, for the values of d and α we seek to obtain, the two-fold PDF of the synthesized set of data will be similar to that of the set of data $\{D_j(x)\}_{j=1,K}$, observed for the double star (the number of scans K and N are not necessarily equal). In practice, this similarity will be quantitatively estimated by computing a distance function $\mathcal{D}(d,\alpha)$ between the observed and synthesized PDFs. This function is expected to have an absolute minimum for the good values of d and α.

To construct the set of speckle images $\{D_i^{d,\alpha}(x)\}$, we assume isoplanetism, and write the double star speckle pattern as the sum of two shifted and weighted identical point source speckle patterns, of the form :

$$D_i^{d,\alpha}(x) = \frac{1}{1+\alpha}\ S_i(x) + \frac{\alpha}{1+\alpha}\ S_i(x-d) \tag{1}$$

The term $(1+\alpha)$ is a normalizing factor that makes the average value of $D_i^{d,\alpha}(x)$ independent of d and α, and equal to that of $S_i(x)$. As indicated above, that ensures the synthesized scans $D_i^{d,\alpha}(x)$ to be directly comparable with the observed ones $D_j(x)$.

The determination of the shifted term $S_i(x-d)$ can be easily done when d is equal to a multiple of the sampling interval ; otherwise an interpolation of the scans must be made. We have tested three interpolating techniques : a simple linear interpolation, an interpolation making use of a decomposition of the signal on a basis of Forsythe polynomials and an interpolation making use of the properties of the Fourier transform. The best results were found when using this latter technique. The shifted speckle pattern $S_i(x-d)$ is obtained as follows (Carbillet[6]).

We compute the Fourier transform $\hat{S}_i(u)$ of $S_i(x)$, and multiply it by a phase term of the form $\exp -i2\pi ud$; then we take the inverse Fourier transform to recover $S_i(x-d)$.

In order to better fit the statistical properties of the synthesized double star patterns to the observed ones, we must take into account the level of noise present in the data. The noise here is mainly of additive origin. We may write :

$$D(x) = \tilde{D}(x) + n_D(x) \tag{2}$$

where $\tilde{D}(x)$ is the noiseless speckle pattern. It can be easily shown (Ricort et al.[16]) that the effect of this noise is to blur the observed PDFs. We can write :

$$P_D(I_1, I_2; \rho) = P_{\tilde{D}}(I_1, I_2; \rho) * P_{n_D}(I_1, I_2; \rho) \tag{3}$$

where the symbol $*$ stands for convolution, and applies on the variables I_1 and I_2. As a result, the two-fold PDF of the speckle pattern is blurred by the two-fold PDF of the noise. Since the noise levels for the double star and the reference point source have in general different rates of blurring, this may be a source of error if a numerical comparison is done.

A possible way to get rid of this blurring effect may be to deconvolve the PDFs from the noise PDF. This was attempted by Ricort et al.[16] using the algorithm of Richardson and Lucy. Although there is indeed an improvement in the resolution of the PDFs, the unregularized nature of the algorithm amplifies the granularity present in the PDFs and due to statistical fluctuations makes the numerical comparison difficult. We decided to make use of an alternative technique which consists of comparing the two-fold PDFs with the resolution of the lower one. From a practical point of view, this consists of applying a blurring function to the PDF, obtained with the sharpest resolution. In fact, all the PDFs were also smoothed with a small Gaussian function to get rid of the effect of statistical fluctuations.

Several kind of distances between observed and synthesized PDFs have been used :

(i) the Euclidean distance :

$$\mathcal{D}_E(d, \alpha) = \sqrt{\sum_{I_1} \sum_{I_2} [P(I_1, I_2; \rho) - P_{d,\alpha}(I_1, I_2; \rho)]^2} \tag{4}$$

(ii) the Kolmogorov distance (Kailath[8]), that can be written as :

$$\mathcal{D}_K(d, \alpha) = \frac{1}{2} \sum_{I_1} \sum_{I_2} |P(I_1, I_2; \rho) - P_{d,\alpha}(I_1, I_2; \rho)| \tag{5}$$

(iii) the distance proposed by Jeffreys[7] and Matusita[13] , of the form :

$$\mathcal{D}_{JM}(d, \alpha) = \sqrt{\sum_{I_1} \sum_{I_2} [\sqrt{P(I_1, I_2; \rho)} - \sqrt{P_{d,\alpha}(I_1, I_2; \rho)}]^2} \tag{6}$$

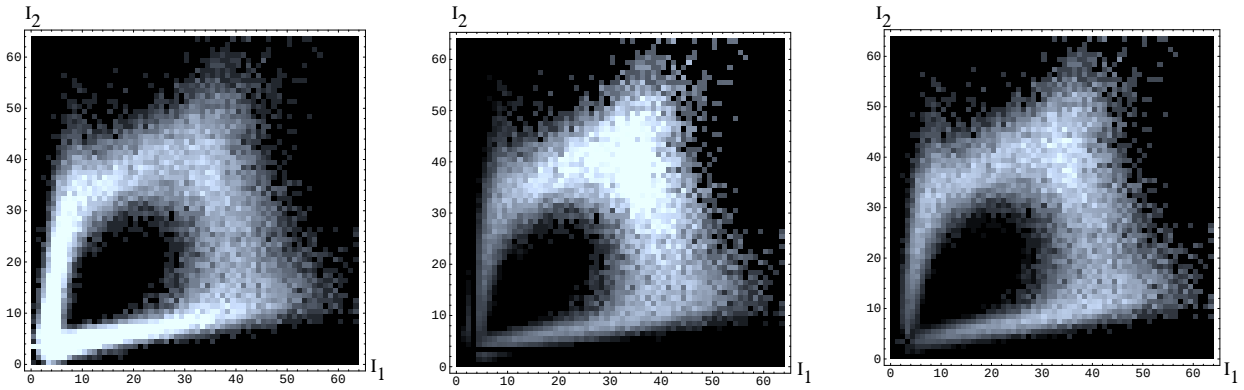

Figure 2: $P(I_1, I_2; \rho = 0''.938)$, $I_1 I_2 P(I_1, I_2; \rho = 0''.938)$ and $(I_1^2 + I_2^2) P(I_1, I_2; \rho = 0''.938)$ for the double star $\zeta\ Aqr$.

(iv) The χ^2 distance proposed by Bédard[5] :

$$\mathcal{D}_{\chi^2}(d, \alpha) = \sum_{I_1} \sum_{I_2} \frac{[P_{d,\alpha}(I_1, I_2; \rho) - P(I_1, I_2; \rho)]^2}{P(I_1, I_2; \rho)} \tag{7}$$

(v) We have also used the Kullback-Leibler distance (Kullback and Leibler[10] ; Titterington[18]), which comes from considerations of entropy :

$$\mathcal{D}_{KL}(d, \alpha) = \sum_{I_1} \sum_{I_2} P_{d,\alpha}(I_1, I_2; \rho)\ \ln\ [\frac{P_{d,\alpha}(I_1, I_2; \rho)}{P(I_1, I_2; \rho)}] \tag{8}$$

As a result, all these distances as they are written in relation 4 to 8 correspond to different quantities and are hardly comparable one to another. Nevertheless, in order to be able to represent them on a same graph, we have made use of a normalizing factor by dividing each of the distances by $\mathcal{D}_*(d, \alpha)$ - with $* = E, K, JM, \chi^2$ or KL - by the distance of $\mathcal{D}_*(d, 0)$ from the observed double star to the reference point source.

In addition to these distances and in order to reduce the influence of the low intensity region (corresponding essentially to the noise present in the data), we made use of two different weighting function that enhance the values of $P(I_1, I_2; \rho)$ for I_1 and I_2 large : $I_1 I_2$ and $(I_1^2 + I_2^2)$ (cf. Figure 2).

3.2 Results

We give in this subsection the results of the determination of d and α for the stars $\zeta\ Aqr$, $\gamma\ Vir$, $\zeta\ Ori$, Gl 473, Gl 866 and Gl 804. In a first part, we apply the whole treatment described in the previous subsection (with all the distances and weighting functions) to the determination of d and α for the star $\zeta\ Aqr$. This will enable us to show the various distances and weighting functions and discuss about their behaviour towards our problem. In a second part, we give the results for the other double stars, with a restricted number of curves.

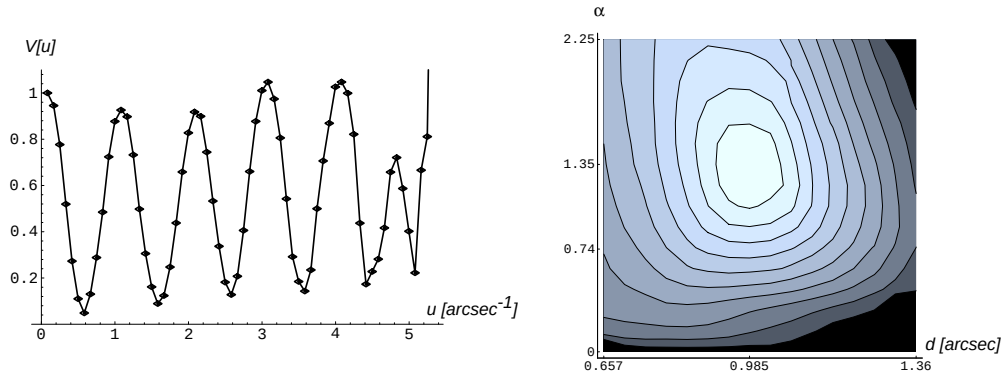

Figure 3: Square visibility function $V[u]$ and Euclidean distance $\mathcal{D}_E(d,\alpha)$ between the PDFs of the double star ζ *Aqr* computed for $\rho = 0''.938$, $d = 0''.655$ to $1''.360$ and $\alpha = 0$ to 2.25. The square visibility function $V[u]$, obtained by dividing the power spectrum calculated for the double star by the one calculated for the reference point source, shows a periodicity that is characterized by the parameters d and α found to be around $0''.985$ for d and around 1.35 or 0.74 for α (since the square visibility function makes no difference between α and $\frac{1}{\alpha}$). The Euclidean distance $\mathcal{D}_E(d,\alpha)$ shows that the good values are around $0''.985$ for d and around 1.35 for α, without ambiguity.

Distance	Euclidean	Kolmogorov	Jeffreys-Matusita	χ^2	Kullback-Leibler
raw PDF	$(0''.9945, 1.28)$	$(0''.9895, 1.36)$	$(0''.9895, 1.36)$	$(0''.9895, 1.36)$	$(0''.9805, 1.36)$
$I_1 I_2$ PDF	$(0''.9805, 1.30)$	$(0''.9895, 1.36)$	$(0''.9895, 1.36)$	$(0''.9895, 1.36)$	$(1''.0040, 1.34)$
$(I_1^2 + I_2^2)$ PDF	$(0''.9805, 1.30)$	$(0''.9895, 1.36)$	$(0''.9755, 1.36)$	$(0''.9895, 1.36)$	$(1''.0040, 1.34)$

Table 1: Results obtained for the 15 distances computed for the binary star ζ *Aqr*. The first number gives the value of the star separation d in units of arcsecond, the second one gives the value of the intensity ratio α.

3.2.1 Detailed analysis for the star ζ *Aqr*

The approach which is described in the previous section consists of finding the values of d and α of the synthesized two-fold PDF that make the distances $\mathcal{D}_*(d,\alpha)$ minimum. Instead of just giving these values for the various $\mathcal{D}_*(d,\alpha)$ considered above, we have found more instructive to represent these functions as two dimensional curves, so that the quality of the various distances may be understood better.

Let us first show how the difference of relative positions of components can be easily obtained from a representation of $\mathcal{D}_*(d,\alpha)$. In Figure 3, we have represented $\mathcal{D}_E(d,\alpha)$ for the double star ζ *Aqr* and a large range of values for d and α. In particular, the variation of α includes the values $\alpha = 1.35$ and $\alpha = 0.74$ which are both acceptable if a power spectrum analysis alone would be done. It is clear in this representation that the minimum of the distance $\mathcal{D}_E(d,\alpha)$ is close to $\alpha = 1.35$, and that for the scanning direction considered, the star of lower intensity is first encountered.

For the same star, we have represented in Figure 4 a two-dimensional representation in gray level of the different distances and weighting functions for a region of the (d,α) plane which is close to the true solution.

In this example, depending of the various distances and weighting functions, we have obtained the results for d and α shown on Table 1.

This table gives an idea of the dispersion of the results. If we consider the sharpness of the determination of

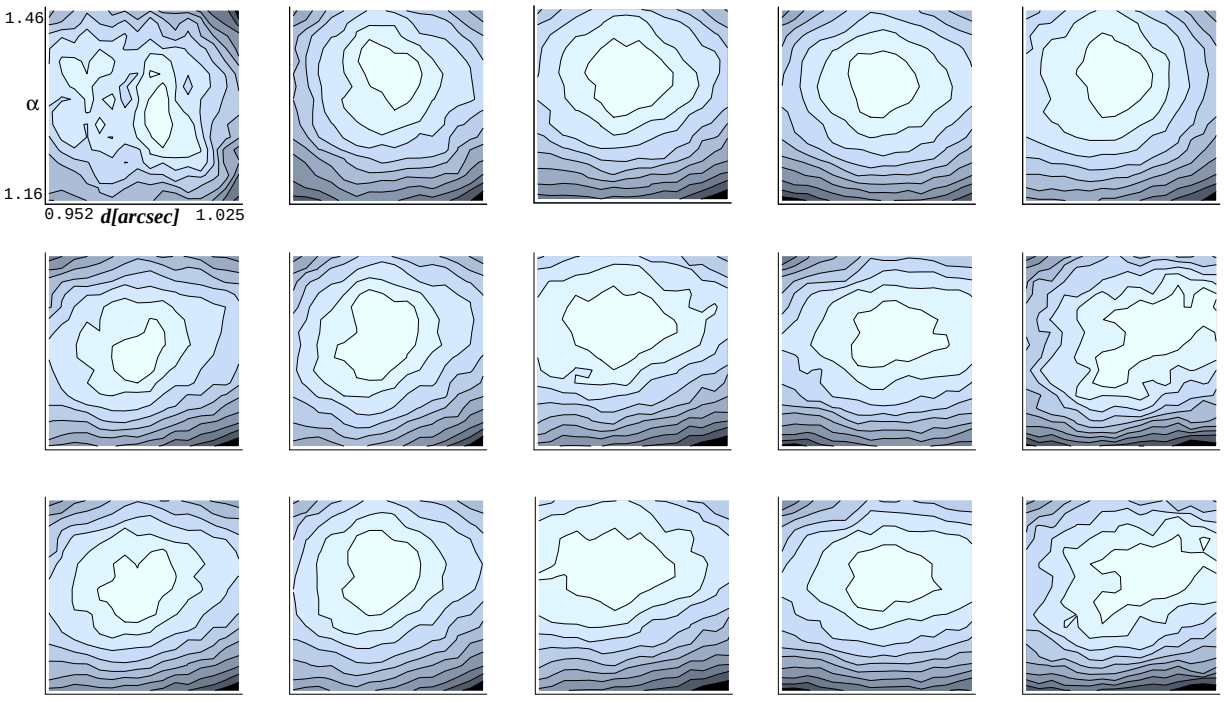

Figure 4: The 15 different distances calculated for a region of the (d, α) plane close to the solution found in the previous Figure. These distances were computed for $\rho = 0\farcs938$, $d = 0\farcs952$ to $1\farcs025$ and $\alpha = 1.16$ to 1.46. From left to right, the columns refer to the Euclidean, Kolmogorov, Jeffreys-Matusita, χ^2 and Kullback-Leibler distances. From top to bottom, the lines consider these distances for the raw PDF, the PDF weighted by $I_1 I_2$, and the PDF weighted by $(I_1^2 + I_2^2)$.

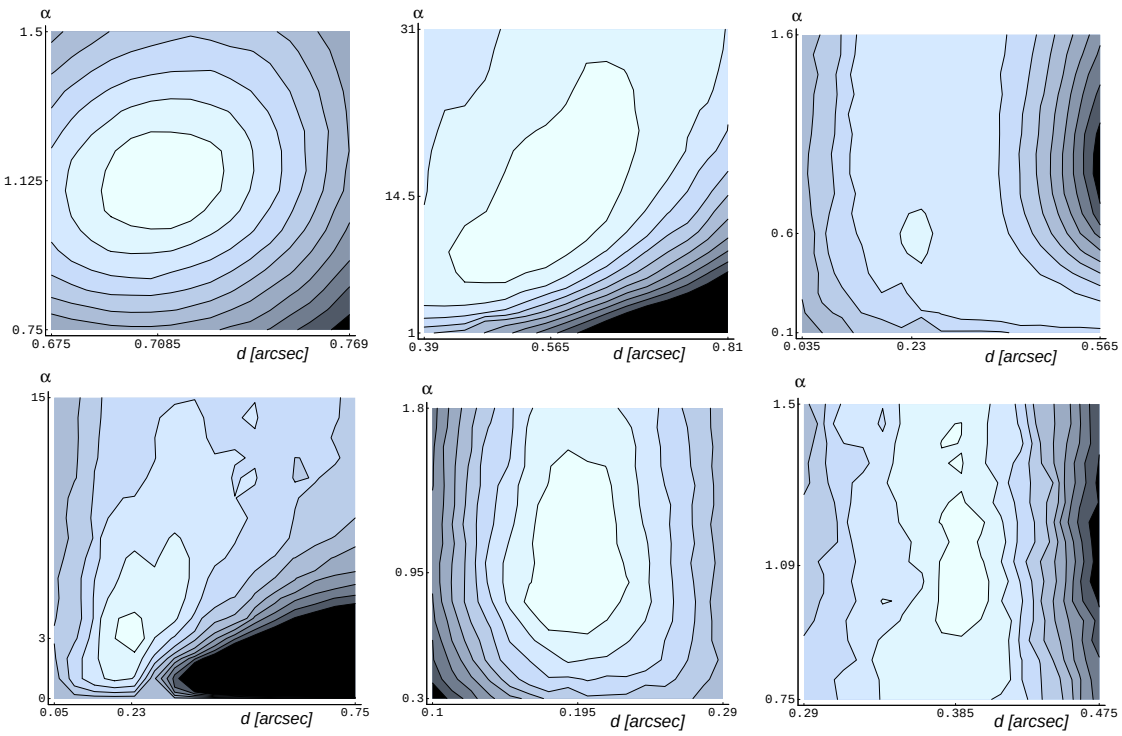

Figure 5: Examples of distance for the sets of scans of five infrared binary stars. From right to left and from top to bottom : Jeffreys-Matusita distance with the $I_1 I_2$ weighting function for $\gamma\ Vir$ computed for $\rho = 0\overset{''}{.}750$, Euclidean distance for $\zeta\ Ori$ computed for $\rho = 0\overset{''}{.}655$, χ^2 distance with the $(I_1^2 + I_2^2)$ weighting function for $Gl\ 866$ computed for $\rho = 0\overset{''}{.}285$, Kolmogorov distance with the $I_1 I_2$ weighting function for $Gl\ 804$ computed for $\rho = 0\overset{''}{.}190$, Kullback-Leibler distance for the first set of data of $Gl\ 473$ computed for $\rho = 0\overset{''}{.}190$, Euclidean distance with the $I_1 I_2$ weighting function for the second set of data of $Gl\ 473$ computed for $\rho = 0\overset{''}{.}375$.

the parameters d and α, we have to exclude the values obtained for the Euclidean distance (fully contaminated by the noise), and the two Kullback-Leibler distances between the weighted PDFs (clearly deteriored here by this kind of operation). So we can write :

$$\begin{cases} d = d_o \overset{+}{-} \sigma_d \ \Rightarrow d = 0\overset{''}{.}9860 \overset{+}{-} 0\overset{''}{.}0055 \\ \alpha = \alpha_o \overset{+}{-} \sigma_\alpha \Rightarrow \alpha = 1.350 \overset{+}{-} 0.025 \end{cases} \tag{9}$$

where d_o and α_o are the average values of d and α, and σ_d and σ_α are the root mean squares of the results obtained in Table 1. We must say however that the quality of these determinations varies from one curve to another depending on the values of d, α, and the noise.

3.2.2 Results for the other binary stars in the near-infrared

The analysis detailed in subsection 3.2.1 is applied here for the double stars $\gamma\ Vir$, $\zeta\ Aqr$, $Gl\ 866$, $Gl\ 804$ and $Gl\ 473$. The first two stars and $\zeta\ Aqr$ are bright double stars, with large orbit periods (856 years for $\zeta\ Aqr$, 171 years for $\gamma\ Vir$ and 1509 years for $\zeta\ Ori$, according to the Sky Catalogue 2000.0[17]). But the last three ones ($Gl\ 866$, $Gl\ 804$ and $Gl\ 473$) are very different. In fact, all of them are less bright, and their orbit periods are

double star	n_o	reference star	n_s	direction	date	separation d	intensity ratio α
$\gamma\ Vir$	654	HR 4837	640	N to S	26/03/1991	$0''.7085 \pm 0''.0035$	1.125 ± 0.025
$\zeta\ Ori$	384	$\epsilon\ Ori$	192	E to W	29/03/1991	$0''.565 \pm 0''.030$	14.5 ± 2
Gl 866	1011	...	256	. to .	10/12/1987	$0''.230 \pm 0''.030$	0.60 ± 0.20
Gl 804	896	HR 7914	480	E to W	28/03/1991	$0''.230 \pm 0''.015$	3.15 ± 0.35
Gl 473#1	893	SRS 42712S	636	N-E to S-W	27/03/1991	$0''.195 \pm 0''.020$	0.95 ± 0.10
Gl 473#2	673	SRS 42712S	328	S-E to N-W	27/03/1991	$0''.3830 \pm 0''.0060$	1.090 ± 0.025

Table 2: Results obtained for the other five infrared double stars in the near-infrared. n_o is the number of scans for the binary star and n_s is the number of scans for the reference star. Scanning direction and date of observation are given, as well as the values and the uncertainties found for the stars separations d and the intensity ratios α.

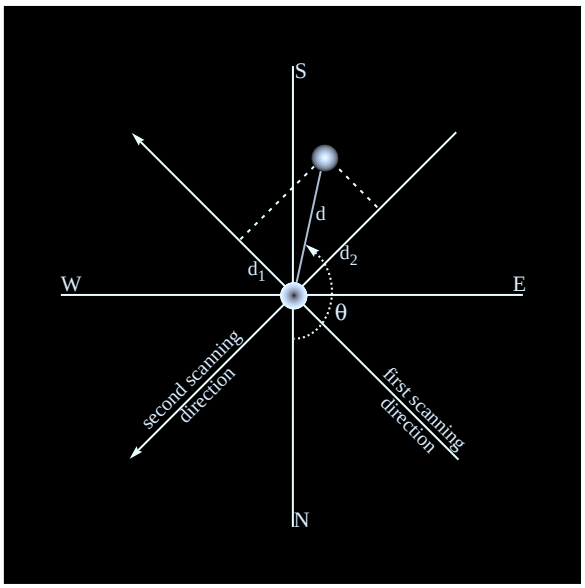

Figure 6: The two scanning directions and the relative position of the two components of Gl 473 (the brightest one being on the center). This figure shows how the PI technique can give a point in the orbit of the observed double star.

shorter : around 2.2 years for Gl 866 (Leinert et al.[12]) and 9.5 years for Gl 473 (Perrier et al.[15]). Observations and results about these objects are therefore more interesting.

We give in Table 2 the results of the determination of d and α obtained for these five binary stars with, for each one, a brief characterization of the data (in mean of number of scans, date of observation and slit direction). We also show, for each star, one of the computed distances (cf. Figure 5). If we consider the two last results for Gl 473 given in Table 2, and by making use of the representation made in Figure 6, we can write for the vector of position $\underline{d}$ (characterized by the separation d and the position angle θ) and the intensity ratio of the brightest star on the lower α :

$$\begin{cases} d = 0''.430 \ \pm \ 0''.015 \\ \theta = (160 \ \pm \ 5)^\circ \\ \alpha = 1.090 \ \pm \ 0.025 \end{cases}$$

4 DISCUSSION

The results we have presented in this paper may bee seen as first quantitative results in PI on one-dimensional images. The first paper published on the double star ζ Aqr (Aime et al.[4]) was a first exploration of the technique, based mainly on a visual inspection of the PDF's curves. The present paper goes further and present a more objective and quantitative analysis, which has the advantage to take into account the state of the atmospheric turbulence through the images of the reference star. The results are in good agreement with the star's ephemerids. The accuracy seems to be remarkable : a few percents for the intensity ratio, the tenth of the diffraction limit for the separation.

Several improvements to this technique may be performed. At present, we compute the distances on a 16×16 grid centered on the supposed minimum. The minimum is then clearly visible on the curves (cf. Figure 4 and Figure 5). This is a lot of useless calculus ; we plan to use an algorithm of minimum searching, for example by steepest descent.

A second improvement may be on the calculation of the uncertainties. They are currently estimated as the standart deviation of the values given by several distances used for each star. A calculus based upon each curve of distance may be more rigorous.

An application of this technique to the visible domain has been tested. But a stronger turbulence made the processing more difficult, and no good results have been yet obtained. In fact, in the visible domain, it is necessary to project the $2D$ specklegrams onto two directions in order to process monodimensional frames. In infrared, this kind of data is directly obtained by scanning the focal plane with a slit, since it did not exist two-dimensional infrared cameras in 1987/1991 (or just prototyps). In the visible, $2D$ images are available and the projections may lower the signal-to-noise ratio. We should obtain better results by computing the PDFs directly on the $2D$ images. The distances would become in that case functions of 3 variables : $\mathcal{D}_*(d_x, d_y, \alpha)$, where d_x and d_y are the components of the separation vector $\underline{d}$.

A possible application to triple stars or more complicated objects may be of interest. But the complexity of the calculation increases quickly. For a triple star, one has to consider distances depending on six parameters and compute more than 16 millions PDFs corresponding to the synthesized triple stars if one want to keep a sampling of 16 points in each direction of the distance function. For an object with N components, the distance functions depend on $3N-3$ parameters, the number of PDFs to compute is then 16^{3N-3}. Thus it should be better to apply another kind of processing in such cases. Aime et al.[2] have shown the existence of a mathematical relation between the two-fold PDF of an object and the three-fold PDF of its point-spread function (reference star). It is probably this kind of analysis that will be used in the future to apply PI to extended objects.

5 ACKNOWLEDGEMENTS

The authors whish to thank Christian Perrier for the data from the ESO infrared slit-scanning specklegraph. Thanks are also due to Henri Lantéri for helpfull discussions about the data processing.

6 REFERENCES

1. C. Aime, "Proposition d'imagerie probabiliste de systèmes d'étoiles en interférométrie de speckle", *J. Opt.(Paris)* **18**, 101–110, 1987.

2. C. Aime, "Probabilistic approach to speckle imaging in optical astronomy", *Trends in Opt. Eng.* **1**, 15–34,

1993.

3. C. Aime and E. Aristidi, "Probability imaging : the statistics of speckle patterns of extended astronomical sources at high light levels", *J. Opt. Soc. Am. A* **8**, 1434–1441, 1991

4. C. Aime, G. Ricort, Ch. Perrier, "Probability imaging of the bright double star ζ Aqr in the infrared", *Exp. Astronomy* **1**, 267–284, 1990

5. G. Bédard, "Analysis of light fluctuations from photon-counting statistics", *J. Opt. Soc. Am. A* **57**, 1201–1206, 1967

6. M. Carbillet, "Détermination des paramètres orbitaux d'étoiles doubles en infra-rouge", internal report, Université de Nice-Sophia Antipolis, France, 1993

7. H. Jeffreys, "An invariant form for the prior probability in estimation problems", *Proc. of the Roy. Soc. A* **186**, 454, 1946

8. T. Kailath, *IEEE Trans.* CT-**15**, 52, 1967

9. T.K. Knox and B.J. Thompson, "Recovery of images from atmospherically degraded short exposures images", *Astrophys. J.* **193**, L45–L48, 1974

10. S. Kullback and R.A. Leibler, "On information and sufficiency", *Ann. Math. Stat.* **22**, 79–86, 1951

11. A. Labeyrie,"Attainment of diffraction-limited resolution in large telescopes by Fourier analysing speckle patterns in star images", *Astron. Astrophys.* **6**, 85–87, 1970

12. Ch. Leinert, M. Haas, F. Allard, R. Wehrse, D.W. McCarthy Jr., H. Jahreiß, Ch. Perrier, "The nearby binary Gliese 866 A/B — Orbit, masses, temperature and composition", *Astron. Astrophys.* **236**, 399–408, 1990

13. K. Matusita, *Ann. Inst. Stat. Math. (Tokyo)* **3**, 17, 1951

14. Ch. Perrier, "ESO infrared specklegraph", *The Messenger* **45**, 29–32, 1986

15. Ch. Perrier, J.M. Mariotti, D. Bonneau, A. Duquennoy, "The orbit of the red-dwarf binary Gliese 473 revisited by speckle interferometry", ESO conf. on *High-Resolution Imaging by Interferometry II*, Beckers J. M. & Merckle F. Eds., Garching-bei-Munchen, Germany, 1991

16. G. Ricort, H. Lantéri, E. Aristidi, C. Aime, "Application of the Richardson-Lucy algorithm to the deconvolution of two-fold probability density functions", *Pure Appl. Opt.* **2**, 125–143, 1993

17. W. Tirion, *Sky Catalogue 2000.0*, vol. 2, Hirshfeld A. & Sinnot R.G. Eds., 1985

18. D.M. Titterington, "General structure of regularization procedures in images reconstruction" *Astron. Astrophys.* **144**, 381–387, 1985

19. G. Weigelt, "Modified speckle interferometry, speckle masking", *Opt. Commun.* **21**, 55–59, 1977